JOURNAL OF NANO- AND ELECTRONIC PHYSICS
Vol. **4** No 3, 03019(5pp) (2012)

ЖУРНАЛ НАНО- ТА ЕЛЕКТРОННОЇ ФІЗИКИ
Том **4** № 3, 03019(5cc) (2012)

Ion Current Density Calculation of the Inductive Radio-Frequency Ion Source

V.I. Voznyi, V.E. Storizhko, V.I. Miroshnichenko, D.P. Shulha

Institute of Applied Physics NAS of Ukraine, 58, Petropavlivska Str., 40030 Sumy, Ukraine

(Received 30 March 2012; in final form 17 September 2012; published online 29 October 2012)

A radio-frequency (RF) inductive ion source at 27,12 MHz is investigated. With a global model of the argon discharge, the plasma density, electron temperature and ion current density of the ion source are calculated in relation to absorbed RF power and gas pressure as a discharge chamber size changes. It is found that ion beam current density grows as the discharge chamber size decreases. Calculations show that in the RF source with a discharge chamber of 30 mm in diameter and 35 mm long the ion current density is 40 mA/cm^2 at 100 W of absorbed RF power and 7 mTorr of pressure, and this agrees well with the experimentally measured value of 43 mA/cm^2. With decreasing discharge chamber diameter to 15 mm ion current density can reach 85 mA/cm^2 at absorbed RF power of 100 W.

Keywords: RF ion source, Ion beam, Plasma, Current density.

PACS numbers: 41.75.Ak, 52.50.Qt, 52.80.Pi

1. INTRODUCTION

Focused ion beams find wide application in micro- and nanotechnologies. For example, in the production of different microdevices it is necessary to manufacture micron-size details. Ion milling is one of the main formation methods of microdetails. During ion milling a part of the work material is sputtered by an ion beam with the energy sufficient for knocking-out of atoms from the material surface. Inert gas argon is mainly used as the source of bombarding ions, since its mass is enough for sputtering and it is rather cheap.

Duoplasmatron and liquid-metal ion source are the most popular ion sources in commercial systems of ion milling [1, 2]. However, these sources have disadvantages, such as the presence of sputtered cathode, impossibility to operate with reactive gases. For ion milling, a plasma radio-frequency (RF) ion source can compete with commercial sources, since it possesses a number of advantages: the absence of sputtered cathode, plasma purity, and possibility to operate with reactive gases.

High brightness of a beam and ion current density of a source are the key parameters of an ion source which define the velocity and productivity of ion treatment. Many scientific groups [3-5] develop RF sources generating ion beams of high brightness. Scientists in IAP NASU study several types of ion RF sources [6-11] in order to increase their brightness. Based on the condition that for the increase in the brightness it is necessary to create a dense plasma in an ion source and extract a beam with high ion current density, a number of ion sources operating at 27,12 MHz was investigated: inductive RF source without external magnetic field (or induction), multicaste RF source with internal antenna and helicon RF source with external magnetic field. The sources were developed to obtain high-brightness beams of H^+ and He^+ easy ions during ion microprobe analysis using electrostatic accelerator complex.

Inductive RF source is the basic one among these sources and has a large potential for further upgrading. For the purpose of application of the inductive RF source in ion milling, consideration of the source operation with working gas Ar and definition of the maximum current density of argon beam are of a great interest.

Estimation of the possibility of increase in the ion beam current density of the inductive RF source with the change in the sizes of its discharge chamber is carried out in the present work. Using the global model of the inductive RF discharge in argon, the plasma parameters of the source and maximum current density of argon beam are determined depending on the absorbed RF power, argon pressure, and sizes of the discharge chamber of the source.

2. THE TECHNIQUE AND THE ION CURRENT DENSITY CALCULATION

The global model of RF discharge is applied for the calculation of the density of ion current extracted from argon plasma of the inductive source [12]. In the model, plasma density n_e and electron temperature T_e are determined from the power balance equation and balance of particles in discharge. It is assumed that density of positive ions and electrons has uniform profile n_e in a whole volume of the discharge excluding the region near walls where particle density drops to the value of n_s. In accordance with the power balance, the total power absorbed by discharge is used for the formation of electron-ion pairs taking into account all elastic and inelastic collisions in the volume. Residual part of the power is lost in the form of the kinetic energy of ions and electrons when they leave discharge to chamber walls. The total power balance is written in the view of [12]

$$P_{abs} = n_s u_b A E_t, \qquad (1)$$

where P_{abs} is the power absorbed by plasma; n_s is the plasma density on the plasma/layer boundary near the wall of discharge chamber; $u_b = (kT_e/M)^{1/2}$ is the Bohm ion velocity on the plasma/layer boundary; k is the Boltzmann constant; T_e is the electron temperature; M is the ion mass; A is the loss area of particles; E_t is the total energy lost by system per one ion.

In order to take into account the difference between the value of n_s on the axial and radial layer boundary, the effective loss area A_{eff} determined from the condition $\int n_s dA = n_e A_{eff}$ (where n_e is the plasma density in the center of discharge) is introduced. For cylinder plasma

discharge with radius R and length L expression for A_{eff} takes the form: $A_{eff} = 2\pi R(Lh_R + Rh_L)$, where $h_L = n_{sL}/n_e$ and $h_R = n_{sR}/n_e$ are the geometric factors equal to the ratio of the axial n_{sL} (and, correspondingly, radial n_{sR}) plasma density on the layer boundary and plasma density in the center. In the middle pressure range when the ion mean free path λ_i is less or of the same order of magnitude than the system sizes, the expressions for h_L and h_R take the form of [12]: $h_L = 0{,}86(3 + L/2\lambda_i)^{-1/2}$, $h_R = 0{,}8(4 + R/\lambda_i)^{-1/2}$. The ion mean free path is equal to $\lambda_i = 1/n_g\sigma_i$, where σ_i is the cross-section of collisions of low-energy ions with neutral atoms in weakly ionized plasma; n_g is the density of neutral gas particles. Two processes, namely, the resonant recharge and elastic scattering, have the maximum scattering cross-sections in the ion-neutral collisions. Total cross-section of these processes is equal to $\sigma_i = 10^{-18}$ m^2 and relatively constant for thermal energies of ions $T_i \sim 0{,}05$ eV. Since density of neutral gas particles depends on the gas pressure p (mTorr) as $n_g = 3{,}3 \cdot 10^{19}\, p$, m^{-3}, then the ion mean free path in collisions with neutral argon atoms is equal to $\lambda_i = 1/33\, p$, m [12].

Solving equation (1), we obtain the average plasma density n_e inside the charge [12]

$$n_e = P_{abs}/u_b A_{eff} E_t. \quad (2)$$

The total loss energy E_t per one ion is defined as [12]: $E_t = E_{ew} + E_{iw} + E_c$, where $E_{ew} = 2kT_e$ is the average kinetic electron energy lost on wall; E_{iw} is the average kinetic ion energy lost on wall; E_c is the collision energy necessary for the formation of one electron-ion pair. Energy E_{iw} is equal to the sum of the initial ion energy at its entry into layer and the energy gained by an ion during acceleration in a layer by the potential difference V_s. Energy of an ion which enters a layer is equal to the Bohm velocity u_b, which corresponds to the directional energy $kT_e/2$. Thus, $E_{iw} = eV_s + kT_e/2$, where e is the electron charge. For the discharge with isolated walls, potential difference V_s between plasma boundary and wall surface is defined from the condition of equality of electron and ion fluxes on isolated surface, whence $V_s = (kT_e/2e)ln(M/2\pi m_e)$, where m_e is the electron mass. For argon $V_s = 4{,}7(kT_e/e)$, therefore, the average kinetic energy of argon ion lost on wall is equal to $E_{iw} \approx 5{,}2kT_e$. Thus, the total loss energy E_t per one ion is equal to $E_t \approx E_c + 7{,}2kT_e$ [12].

Collision energy E_c necessary for the formation of one electron-ion pair is determined as [12]

$$E_c = E_{iz} + \sum[E_{ex,i}(K_{ex,i}/K_{iz}) + (K_{el}/K_{iz})(2m_e/M)(3kT_e/2)], \quad (3)$$

where E_{iz}=15,76 eV is the ionization energy of argon atom; $E_{ex,i}$ is the threshold excitation energy of the i-th atomic level; K_{iz} is the rate constant of ionization; $K_{ex,i}$ is the rate constant of excitation of the i-th atomic level; K_{el} is the rate constant of elastic scattering of electrons on neutral atoms.

Equation (3) takes into account the electron energy losses due to ionization, excitation, and elastic scattering on neutral atoms. These are the main energy losses in weakly ionized electropositive discharges. The value of $(2m_e/M)(3kT_e/2)$ is the average energy lost by an electron at elastic collision with an atom. Using the values of the constants K_{iz}, $K_{ex,i}$, and K_{el} for argon depending on the electron temperature [12], one can define the energy ε_c necessary for the formation of one electron-ion pair.

The electron temperature T_e is determined from the particle balance equation in discharge. The total loss of electrons and ions on the surface of discharge chamber is balanced by the formation of electron-ion pairs as a result of ionization inside plasma volume. For cylinder discharge chamber with the radius R and length L the particle balance equation has the form of [12]

$$K_{iz}/u_b = 1/n_g d_{eff}, \quad (4)$$

where $d_{eff} = 0{,}5RL/(Lh_R + Rh_L)$ is the effective plasma size. Using the rate constant of ionization of neutrals by electrons K_{iz}, equation (4) is solved with respect to T_e for the given values of n_g and d_{eff} and, thus, the electron temperature T_e is defined depending on the pressure p. Having determined the electron temperature, one can find the formation energy of electron-ion pair E_c and calculate the total loss energy E_t per one ion subject to the gas pressure. Using equation (2), one can determine the plasma density depending on the gas pressure and absorbed power.

The maximum density of ion current which can be extracted from plasma with the density n_e and electron temperature T_e in the absence of the external magnetic field is the saturation current density j_s. During extraction of the current, j_s is defined by the ion density n_s on the plasma-layer boundary and Bohm ion velocity u_b:

$$j_s = en_s u_b = en_e h_L (kT_e/M)^{1/2}. \quad (5)$$

3. EXPERIMENTAL EQUIPMENT

General scheme of the inductive RF ion source is illustrated in Fig.1. The source contains cylinder quartz discharge chamber with the outer diameter D and the length L, on which spiral RF antenna (3,5 coils of copper wire of the diameter of 3 mm) is located. Length of the Mo extractor channel is equal to 3mm and diameter – d = 0,6 mm. The quartz diaphragm is placed between plasma and extractor.

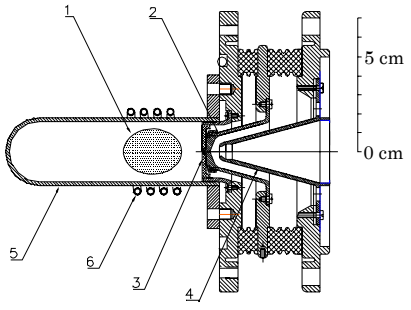

Fig. 1 – Scheme of the inductive RF source: 1 – plasma volume; 2 – extractor; 3 – diaphragm; 4 – focusing electrode; 5 – discharge chamber; 6 – spiral RF antenna

RF system contains the driving generator with the frequency of 27,12 MHz, power amplifier "ACOM-1000" (500 W), and matching system consisting of the load and resonant variable capacitors. Changing the capacitor capacities, one can reach the position when level of the reflected power is close to zero. In this case, the value of the direct power is the RF power P supplied to the source discharge.

Vacuum chamber of the plant is pumped out by the turbo-molecular pump "Leybold-350" providing pressure on the level of $4 \cdot 10^{-6}$ Torr. Gas puffing system "CHA-2" is used for Ar puffing into the ion source.

4. RESULTS AND DISCUSSION

4.1 Results of the ion current density calculation

The plasma density n_e, electron temperature T_e, and ion saturation current density j_s for the inductive RF source with cylinder discharge chamber of the diameter $D = 2R$ and length L were calculated solving equations (2)-(5). Calculations were performed for four variants of chamber sizes: 1) $D = 30$ mm, $L = 70$ mm, 2) $D = 30$ mm, $L = 35$ mm, 3) $D = 15$ mm, $L = 70$ mm, 4) $D = 15$ mm, $L = 35$ mm. Argon pressure in the source chamber was changed in the range of 1-50 mTorr.

Dependence of the electron temperature T_e on the argon pressure p in discharge is represented in Fig. 2 for four variants of discharge chamber sizes D and L. It is seen from Fig. 2 that at the increase in the pressure from 1 to 50 mTorr, electron temperature T_e decreases monotonously from 8,5 eV to 2,2 eV. At the decrease in the discharge chamber length L from 70 mm to 35 mm, electron temperature T_e is weakly changed. A larger change in the temperature occurs at the decrease in the chamber diameter D. In the chamber with the diameter $D = 30$ mm and the length $L = 35$ mm at the pressure $p = 6$-10 mTorr, electron temperature is $T_e = 3,5$-4 eV.

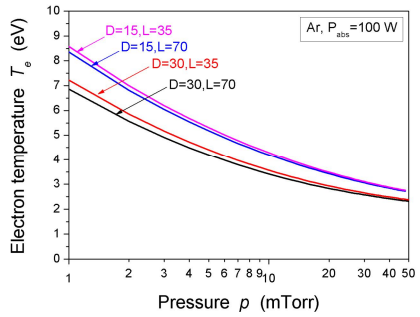

Fig. 2 – Dependence of the electron temperature T_e on the Ar pressure p for four variants of discharge chamber sizes

According to equation (2), the plasma density n_e is directly proportional to the absorbed RF power P_{abs}. Taking into account this fact, the calculation results of the plasma density and ion saturation current density are given for the power value of $P_{abs} = 100$ W. In order to find n_e and j_s for large values of RF power, it is necessary to proportionally increase the specified values. RF power P_{abs} absorbed by discharge is determined as $P_{abs} = \eta P$, where P is the power supplied to discharge; η is the efficient factor of power introduction into plasma. Determination of the efficient factor η is performed in the work [10]. Efficient factor depends on the gas pressure p in discharge, and at the pressure of 7 mTorr efficient coefficient η is equal to 0,83 in a wide range of RF power P supplied to discharge.

In Fig. 3 we present the dependence of the average density of argon plasma n_e on the pressure p for four variants of discharge chamber sizes D and L. It is seen that at the decrease in the length and diameter of the discharge chamber, average plasma density increases. This is explained by the decrease in the surface area A, on which particle loss takes place. In discharge chamber of the diameter $D = 30$ mm and length $L = 35$ mm plasma density monotonously increases from the value of $n_e = 8,8 \cdot 10^{11}$ cm^{-3} to $n_e = 5,5 \cdot 10^{12}$ cm^{-3} at the increase in the gas pressure from 1 to 50 mTorr. At the working Ar pressure of $p = 7$ mTorr, average plasma density is equal to $n_e = 2,5 \cdot 10^{11}$ cm^{-3}. In the chamber with diameter of 15 mm at the same gas pressure plasma density increases to $n_e = 4,9 \cdot 10^{12}$ cm^{-3}.

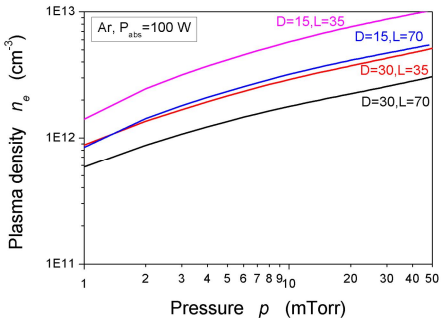

Fig. 3 – Plasma density n_e versus the Ar pressure p for four variants of discharge chamber sizes D and L. $P_{abs} = 100$ W

Ion saturation current density j_s, which can be extracted from plasma discharge, is defined by equation (5) and proportional to the value of the absorbed RF power P_{abs}. In Fig. 4 we present the calculation results of the dependence of the ion saturation current density j_s on the gas pressure p for four variants of discharge chamber sizes D and L. At the increase in the argon pressure from 1 to 50 mTorr, ion saturation current density increases, reaches the maximum, and then drops. This is explained by the fact that current density j_s is the product of functions one of which – the plasma density n_e – increases with pressure growth, and other – u_b and h_L – decrease.

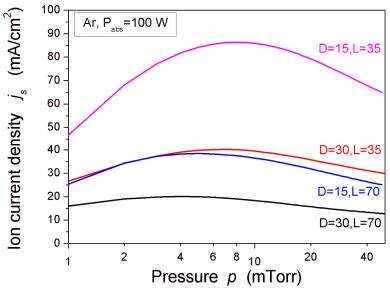

Fig. 4 – Dependence of the ion saturation current density j_s on the argon pressure p for four variants of discharge chamber sizes D, L. $P_{abs} = 100$ W

As seen from Fig. 4, at the decrease in the discharge chamber sizes ion saturation current density increases. The gas pressure, at which current density reaches the maximum, slightly increases. In the discharge chamber of the diameter $D = 30$ mm and length $L = 70$ mm, the maximum current density is equal to $j_i = 20$ mA/cm^2 at the gas pressure $p = 3$-5 mTorr. At the decrease in the chamber length to $L = 35$ mm, the maximum current density increases to $j_i = 40$ mA/cm^2. The same ion current density can be obtained in the discharge chamber of the diameter $D = 15$ mm and length $L = 70$ mm. At

the decrease in the chamber length to $L = 35$ mm, the maximum current density can increase to the value of $j_i = 85$ mA/cm^2.

4.2 Measurements of the ion current density

In the plasma source, ions formed in the discharge chamber drifting reach the region of extraction and are extracted by the extraction voltage V_{ext}. In the RF source emitting boundary is not fixed (see Fig. 5). At the given geometry of extractor plasma density should be consistent with the value of the extraction voltage [13, 14]. The shape and position of the emitting boundary are determined by the balance between density of ion flux from plasma (saturation current density j_s) and density of current j_c limited by a space charge. Current density j_c is defined by the Child-Lengmur law [13]

$$j_c = (4\varepsilon_0/9)(2q/M)^{1/2}(V_{ext}^{3/2}/s^2), \quad (6)$$

where ε_0 is the dielectric constant; q is the ion charge; V_{ext} is the extraction voltage; s is the distance between extractor and plasma boundary.

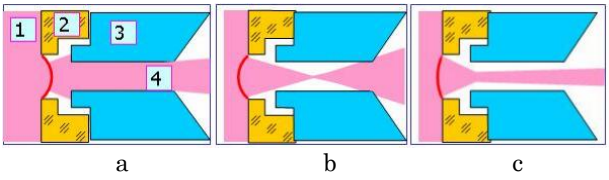

Fig. 5 – Shape of an ion beam extracted from the plasma RF source: 1 – plasma; 2 – insulator; 3 – extractor; 4 – beam

Thus, position of the plasma boundary is defined by the correlation between plasma density n_e and extraction voltage V_{ext}. At large plasma density (or small V_{ext}) plasma boundary is convex (Fig. 5a); beam is underfocused and beam divergence is large; distance s between plasma boundary and extraction electrode is small; a considerable part of a beam reaches extractor. At small plasma density (or large V_{ext}) plasma boundary is concave (Fig. 5b), beam is overfocused and divergent; part of a beam reaches extractor. When outgoing beam is consistent with extraction system, then its divergence is not large and beam is almost parallel (Fig. 5c).

In Fig. 6 we represent the measurement results of the ion current density of a beam extracted from the inductive RF source. Ion current density j_i was defined by the ratio of the total beam current I_i to the extractor orifice area: $j_i = 4I_i/\pi d^2$, where $d = 0{,}6$mm is the extractor hole diameter. Ion current I_i was measured using the Faraday cylinder with suppressor for the suppression of the secondary ion current.

Dependence of the current density of argon beam j_i versus the extraction voltage V_{ext} is shown in Fig. 6. As seen, current density j_i increases with the rise of the extraction voltage V_{ext} (formula (6)) and at the values of $V_{ext} = 1{,}6$-$2{,}4$ kV it reaches saturation (see formula (5)). At the input power $P = 120$ W and the argon pressure $p = 7$ mTorr the maximum current density is equal to 43 mA/cm^2 that agrees well with the calculated value 40 mA/cm^2.

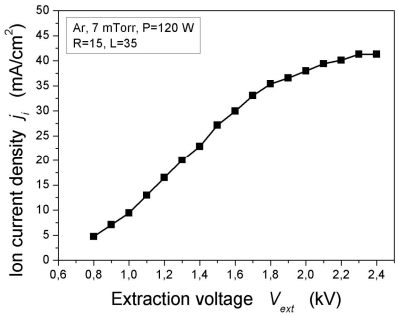

Fig. 6 – Ion current density j_i subject to the extraction voltage V_{ext}. $D = 30$ mm, $L = 35$ mm, $p = 7$ mTorr, $P = 120$ W

5. CONCLUSIONS

We have considered the work of the inductive ion RF source without magnetic field for the using in ion milling. Based on the global model of the inductive RF discharge in argon, the plasma parameters of the source and the maximum current density of argon beam are determined versus the absorbed RF power, argon pressure, and discharge chamber sizes. It is established that the maximum ion current density is proportional to the RF power absorbed by discharge and increases with the decrease in the discharge chamber sizes.

For steady operation of the source, reduction of its temperature regime, and decrease in the RF leakage on the measurement equipment, one should not increase RF power more than ~ 150 W. Therefore, increase in the ion current density due to the decrease in the size of the source discharge chamber is of an interest. Calculations have shown that in the chamber of the diameter $D = 30$ mm and length $L = 35$ mm the maximum ion current density is equal to 40 mA/cm^2 at $P_{abs} = 100$ W.

We have carried out the measurements of the current density of argon beam from discharge chamber of such sizes and obtained the value of 43 mA/cm^2 that confirms the correctness of the performed calculations. It is established that at the decrease in the chamber diameter to $D = 15$ mm ion current density can reach the value of 85 mA/cm^2 at 100 W of RF power, and, so, ~ 120 mA/cm^2 at $P_{abs} = 150$ W. Further decrease in the discharge chamber diameter is not reasonable, since in this case geometric sizes of RF antenna decrease and the RF power input to discharge becomes more complex. Thus, for the extraction of high-density current from inductiven RF source without external magnetic field, the optimal sizes of discharge chamber are the following: diameter $D = 15$-20 mm and length $L = 30$-35 mm.

REFERENCES

1. C.D. Coath, J.V.P. Long, *Rev. Sci. Instrum.* **66**, 1018 (1995).
2. R. Clampitt, D.K. Jefferies, *Nucl. Instrum. Meth.* **149**, 739 (1978).
3. N.S. Smith, P.P. Tesch, N.P. Martin, D.E. Kinion, *Appl. Surf. Sci.* **255**, 1606 (2008).
4. X. Jiang, Q. Ji, A. Chang, K.N. Leung, *Rev. Sci. Instrum.* **74**, 2288 (2003).
5. Y.J. Kim, D.H. Park, H.S. Jeong, Y.S. Hwang, *Rev. Sci. Instrum.* **77**, 03B507 (2006).
6. V.I. Miroshnichenko, S.N. Mordik, V.V. Olshansky, K.N. Ste-

panov, V.E. Storizhko, B. Sulkio-Cleff, V.I. Voznyy, *Nucl. Instrum. Meth. B* **201**, 630 (2003).
7. V.I. Voznyy, V.I. Miroshnichenko, S.N. Mordyk, A.G. Nagornyy, D.A. Nagornyy, V.E. Storizhko, D.P. Shulha, *Probl. At. Sci. Tech. Ser.: Plasma Physics* **10** No1, 209 (2005).
8. V. Miroshnichenko, S. Mordyk, D. Shulha, V. Storizhko, V. Voznyy, *Nucl. Instrum. Meth. B* **260**, 39 (2007).
9. S. Mordyk, V. Miroshnichenko, D. Shulha, V. Storizhko, *Rev. Sci. Instrum.* **79**, 02B707 (2008).
10. V. Voznyi, *J. Nano-Electron. Phys.* **2** No2, 75 (2010).
11. V.I. Voznyi, V.I. Miroshnichenko, S.N. Mordik, A.G. Nagornyy, D.A. Nagornyy, V.E. Storizhko, D.P. Shulha, *Nauka ta innovatsii* **6** No5, 38 (2010).
12. M.A. Lieberman, A.J. Lichtenberg, *Principles of Plasma Discharges and Materials Processing*. (New York: Wiley: 1994).
13. B.H. Wolf, *Handbook of Ion Sources*. (Boca Raton: CRC Press: 1995).
14. P. Spadtke, *Rev. Sci. Instrum.* **63**, 2647 (1992).